

# Non-parametric estimation of Fisher information from real data

Omri Har Shemesh,<sup>1,\*</sup> Rick Quax,<sup>1,†</sup> Borja Miñano,<sup>2,‡</sup> Alfons G. Hoekstra,<sup>1,3,§</sup> and Peter M.A. Sloot<sup>1,3,4,¶</sup>

<sup>1</sup>*Computational Science Lab, University of Amsterdam,  
Science Park 904, 1098XH, Amsterdam, The Netherlands*

<sup>2</sup>*IAC<sup>3</sup> UIB, Mateu Orfila, Cra. de Valldemossa km 7.5, 07122, Palma, Spain*

<sup>3</sup>*ITMO University, Saint Petersburg, Russia*

<sup>4</sup>*Complexity Institute, Nanyang Technological University,  
60 Nanyang View, Singapore 639673, Republic of Singapore*

(Dated: December 7, 2024)

The Fisher Information matrix is a widely used measure for applications ranging from statistical inference, information geometry, experiment design, to the study of criticality in biological systems. Yet there is no commonly accepted non-parametric algorithm to estimate it from real data. In this rapid communication we show how to accurately estimate the Fisher information in a non-parametric way. We also develop a numerical procedure to minimize the errors by choosing the interval of the finite difference scheme necessary to compute the derivatives in the definition of the Fisher information. Our method uses the recently published “Density Estimation using Field Theory” algorithm to compute the probability density functions for continuous densities. We use the Fisher information of the normal distribution to validate our method and as an example we compute the temperature component of the Fisher Information Matrix in the two dimensional Ising model and show that it obeys the expected relation to the heat capacity and therefore peaks at the phase transition at the correct critical temperature.

PACS numbers: 02.60.-x,05.10.-a,05.50.+q,64.60.-i

Consider a probabilistic description of a system as a probability density function (PDF)  $p(x; \theta)$ . The observables of the system are collected as parts of the vector  $x$  and the PDF will typically depend on a vector of continuous parameters  $\theta$ . We are often interested in how the system responds to changes in these parameters, e.g. to study phase transitions or the dynamics of the system in the vicinity of bifurcations. A measure of the sensitivity of the PDF to the parameters is the Fisher Information Matrix (FIM) [1]. It is a symmetric matrix whose entries are labeled by the parameters of the PDF. If a small parameter change causes a large change in the PDF, the corresponding entry in the FIM will be large. There is a vast literature about the different uses of the FIM which we cannot hope to cover here. We wish to highlight, however, its interpretation as a Riemmanian metric on the statistical manifold [2] and its relation to the theory of phase transitions in physics [3–12] and complex systems [13–19].

Since the FIM is directly computed from the PDF, its accurate estimation depends on the more general problem of density estimation [20]. Density estimation aims to obtain the best estimate  $Q_{\text{est}}$  of a distribution  $Q_{\text{true}}$  given  $N$  samples that are independently drawn from it. We distinguish between parametric and non-parametric estimation. Parametric estimates constrain the form of the estimated density  $Q_{\text{est}}$  to depend on a few parameters

that that are then estimated from the data using appropriate methods [21]. Since by the Cramér-Rao inequality [1] the inverse of the Fisher information is a lower-bound on the variance of the estimated parameters, a large portion of the literature in which Fisher information is computed is concerned with the parametric estimation problem. In these cases the Fisher information is computed analytically from the assumed function.

When we do not wish to assume a specific form for the PDF, we estimate the density non-parametrically. The main idea behind the non-parametric methods is to let the data determine the shape of the distribution. It is assumed that areas with higher probability density will contain more data points than areas with lower probability. The main problem that the non-parametric methods face is how to balance the goodness of fit to the data and the smoothness of the estimated curve [20]. For example, kernel density estimators (KDEs) are a sum over kernel functions with width  $h$  that are positioned at each data point. i.e.  $Q_{\text{est}}(x) = (hN)^{-1} \sum_{i=1}^N K[(x - x_i)/h]$  where  $x_i$  is a data point and  $K$  is a kernel function. The parameter  $h$ , called the bandwidth, controls the smoothness of the estimate. In the limit  $h \rightarrow 0$  the estimate is a sum of delta functions placed at each data point; in the  $h \rightarrow \infty$  it is a uniform distribution. This illustrates the importance of the right choice of a bandwidth parameter. Taken too large and the estimate will hide crucial features while a too small bandwidth causes spurious peaks in the data to appear, especially for long-tailed distributions [20]. Important to this study, the amount of smoothing in the estimate directly affects the value of the Fisher informa-

\* Electronic mail: O.HarShemesh@uva.nl

† Electronic mail: R.Quax@uva.nl

‡ Electronic mail: bminyano@mail.iac3.eu

§ Electronic mail: A.G.Hoekstra@uva.nl

¶ Electronic mail: P.M.A.Sloot@uva.nl

tion. This can be seen in its definition:

$$g_{\mu\nu}(\theta) = \langle (\partial_\mu \ln p)(\partial_\nu \ln p) \rangle, \quad (1)$$

which depends on the derivatives of the PDF. Here  $\partial_\mu \equiv \partial/\partial\theta^\mu$ ,  $p$  is a PDF and the average is with respect to  $p$ . If, e.g. the estimated PDF  $Q_{\text{est}}$  is smoother than the true PDF  $Q_{\text{true}}$ , the estimate for the Fisher information will be smaller than the true Fisher information.

One elegant approach that lets the smoothness be derived from the data itself was first proposed in [22]. They used field theory to formulate the notion of a smoothness scale as an ultraviolet cutoff, and treated the smoothness length scale  $\ell$  as a parameter in a Bayesian inference procedure. They were able to show that, in the large  $N$  limit, the data will select an appropriate length scale. Recently this method was developed further and a fast and accurate algorithm called DEFT (Density Estimation using Field Theory) was published [23]. The algorithm was implemented in one and two dimensions, since, as many other methods, it suffers from the ‘‘curse of dimensionality’’ [23]. In the current work we will use DEFT as a way to obtain a PDF from samples taken at various values of the parameters  $\theta$  and compare the results for the Fisher computation with the results we obtain by using KDE.

Previous work on nonparametric estimation of the Fisher information primarily dealt with PDFs whose dependence on the parameters is as a location parameter, i.e.  $p(x; \theta) = p(x - \theta)$ . In that setting Huber [24] found a unique interpolation of the cumulative distribution function that maximizes the Fisher information. Kostal and Pokora [25] suggested an adaptation of the maximized penalized likelihood method of Goodd and Gaskins [26] to compute the Fisher information. Kostal and Pokora rejected the use of KDE for the direct computation of the Fisher Information because of the lack of control of the  $p'/p$  term in its definition [25]. To show that using DEFT does indeed produce better results we will compare the two methods (KDE and DEFT) by using both to compute the Fisher information of the normal distribution, which is known analytically. We will then compute the Fisher information in the two dimensional Ising model and show that it is able to detect the critical temperature as expected.

To proceed we replace the derivatives in Eq. (1) with centered finite-difference derivatives:

$$g_{\mu\nu}(\theta) \approx \int \frac{p(x; \theta + \Delta\theta^\mu) - p(x; \theta - \Delta\theta^\mu)}{2\Delta\theta^\mu} \times \frac{p(x; \theta + \Delta\theta^\nu) - p(x; \theta - \Delta\theta^\nu)}{2\Delta\theta^\nu} \frac{dx}{p(x; \theta)}. \quad (2)$$

Here  $\Delta\theta^\mu$  indicates a change in the value of only one parameter  $\theta^\mu$  keeping all other parameters fixed, i.e.,  $\theta + \Delta\theta^\mu \equiv (\theta^1, \dots, \theta^\mu + \Delta\theta^\mu, \dots, \theta^d)$ . The error introduced by this replacement is proportional to  $O(\Delta\theta^2/6)$  (for each derivative) as can be verified by Taylor expansion. It is possible to use higher order finite-difference schemes but not, in our experience, a lower order one-sided derivative

because in that case the estimate does not converge to the true value (data not shown). For the purpose of this paper the centered derivative is sufficient.

This introduces a new free parameter: the size of the difference  $\Delta\theta^\mu$ . Fixing the value of  $\Delta\theta^\mu$  has a large influence on the accuracy of the computation. There are two sources of error that determine the optimal value of  $\Delta\theta^\mu$ : the aforementioned error in the numerical derivative and the finite sample size  $N$ . The first error, which scales like  $O[(\Delta\theta^\mu)^2]$ , becomes smaller with decreasing  $\Delta\theta$ . The second source, however, is minimized when we increase  $\Delta\theta^\mu$ . This happens because a density estimate with a finite number of samples is always under-determined. Any estimate will produce a curve that is one of a group of curves that are close to the true density, but not exactly the same. The larger the number of samples, the smaller the size of the group of curves. If  $\Delta\theta^\mu$  is too small, the groups of close curves of the two densities in the numerical derivatives will overlap and the difference  $p(x; \theta + \Delta\theta^\mu) - p(x; \theta - \Delta\theta^\mu)$  will be ill-defined. This leads us to one of our main results: since  $\Delta\theta^\mu$  cannot be too small or too large, there is some optimal value between the two extremes where the error is minimal.

To estimate the size of the groups of curves and make sure they don’t overlap we can use large deviations theory. According to Sanov’s theorem [27] the appropriate distance measure is the Kullback-Leibler divergence:

$$\mathcal{D}_{KL}[Q||P] \equiv \int_{x \in \mathcal{X}} Q(x) \ln \frac{Q(x)}{P(x)} dx \quad (3)$$

which is defined for two densities  $P(x)$  and  $Q(x)$  where the support of  $P$  overlaps the support of  $Q$ . Roughly speaking, the probability of a set of  $N$  samples that are independently drawn from  $P$  to appear to be drawn from  $Q$  is proportional to:

$$\exp(-N\mathcal{D}_{KL}[Q||P]). \quad (4)$$

In the limit of infinite sample size this probability goes to zero. For finite  $N$  there is a set of distributions whose KL-divergence with  $P$  is small enough such that this probability is not negligible. This set can be interpreted as a hypersphere in parameter space centered at  $\theta$  with an  $N$ -dependent radius. For maximum accuracy we require that the radius of the spheres at  $\theta$  and  $\theta + \Delta\theta^\mu$  should be small compared to their separation  $\Delta\theta^\mu$ . Fig. 1 shows a schematic plot of this in one dimension. Fig. 1a represents the ideal case of well separated densities and Fig. 1b is one where  $\Delta\theta^\mu$  is too small for the number of samples  $N$ .

To compute the radius of the hypersphere we take  $P = p(x; \theta)$  and  $Q = p(x; \theta + \varepsilon\Delta\theta^\mu)$  in Eq. (4). This effectively means that we seek the density  $Q$  at the edge of the hypersphere and parametrize it with  $\varepsilon$  that is effectively the radius of the hypersphere in units of  $\Delta\theta^\mu$ . The KL-divergence of two close distributions can be approximated

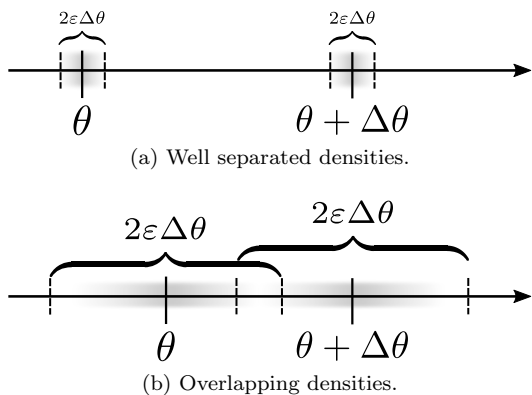


FIG. 1. Two examples of the one dimensional parameter space with points of estimation  $\theta$  and  $\theta + \Delta\theta$ . The gray area is the hypersphere described in the text.  $\varepsilon$  is the radius of the hypersphere in units of  $\Delta\theta$ .

by the Fisher distance between them:

$$\mathcal{D}_{KL}[P(\theta)||P(\theta + \varepsilon\Delta\theta^\mu)] \approx \frac{\varepsilon^2}{2} g_{\mu\nu}(\theta) \Delta\theta^\mu \Delta\theta^\nu = O(\Delta\theta^2) \quad (5)$$

where we use the Einstein summation convention for repeated indices [28]. Inserting Eq. (5) into Eq. (4) we get

$$\exp\left[-\frac{N\varepsilon^2}{2} g_{\mu\nu}(\theta) \Delta\theta^\mu \Delta\theta^\nu\right]. \quad (6)$$

We choose the point where the probability is equal to  $e^{-1}$  as the boundary of the hypersphere. This is an arbitrary choice and a different choice will lead to a rescaling of  $\varepsilon$  by a constant factor. Equating Eq. (6) with  $e^{-1}$ , we obtain the radius  $\varepsilon$ :

$$\varepsilon^2 = \frac{2}{N g_{\mu\nu}(\theta) \Delta\theta^\mu \Delta\theta^\nu}. \quad (7)$$

As expected, two factors influence the radius: the number of samples  $N$  and  $\Delta\theta^\mu$ . At a given  $N$  and  $\theta$ , *increasing*  $\Delta\theta^\mu$  will *decrease* the radius and thus increase accuracy.

As an example, which can be solved both analytically and numerically, we take the univariate normal distribution  $\mathcal{N}(\mu, \sigma)$ . Its Fisher information is

$$g_{\mu\mu} = \frac{1}{\sigma^2}; \quad g_{\sigma\sigma} = \frac{2}{\sigma^2}; \quad g_{\mu\sigma} = g_{\sigma\mu} = 0. \quad (8)$$

The Fisher information matrix is diagonal and depends only on  $\sigma$ . We focus specifically on the  $g_{\sigma\sigma}$  component, which corresponds to  $\sigma$  which is not a location parameter. Inserting this to Eq. (7) gives

$$\Delta\sigma = \sqrt{\frac{2}{\varepsilon^2 N g_{\sigma\sigma}}} = \frac{\sigma}{\varepsilon\sqrt{N}}, \quad (9)$$

where we defined  $\Delta\sigma = \Delta\theta^\sigma$ . This tells us which  $\Delta\sigma$  is appropriate for a given  $N$  and  $\sigma$ . We can also obtain this result in a different way. According to the Cramér-Rao

inequality, the minimal variance of an unbiased estimator for  $\sigma$  is  $1/g_{\sigma\sigma}$ . For  $N$  samples this is equal to  $\sigma^2/2N$ . Assume we use an estimator with minimal variance and demand that the variance of  $\sigma$  is equal to  $\frac{1}{2}(\varepsilon\Delta\sigma)^2$  (the factor  $\frac{1}{2}$  is for a consistent definition of  $\varepsilon$ ). The choice of this variance is equivalent to setting a hypersphere radius of  $\varepsilon\Delta\sigma$ . We then have  $\sigma^2/2N = (\varepsilon\Delta\sigma)^2/2$ . Solving for  $\Delta\sigma$  gives Eq. (9).

For real data the Fisher information is unknown. We propose to use  $\varepsilon$  in an iterative way. First compute the Fisher information with values of  $\Delta\theta^\mu$  that ensure a good approximation of the numerical derivatives. Then use the Fisher information to compute  $\varepsilon$ . If it is too large ( $\varepsilon \approx 0.1$  seems to be a reasonable value), increase  $\Delta\theta^\mu$  (by sampling a different point in parameter space) or increase the number of samples  $N$  and repeat the computation. This depends on the specific case.

We demonstrate our main results by computing the Fisher information  $g_{\sigma\sigma}$  from samples drawn independently from the normal distribution. We first compare the performance of two density estimation algorithms: DEFT (with number of grid points  $G = 100$ , smoothness parameter  $\alpha = 3$  and a bounding box twice the interval between the smallest and largest sample [23]) and KDE (using Scott's rule to determine the bandwidth). We used both DEFT and KDE to get a density estimation from the same samples and computed the Fisher information using equation (2). In the top plot of Fig. 2 the Fisher information, in logarithmic scale, is shown. The black curve is the analytic value  $2/\sigma^2$ , the green dots and blue rectangles are the median estimate out of 100 repetitions (error bars represent 5 and 95 percentiles) for DEFT and KDE respectively. At each  $\sigma$  we used  $N = 10^4$ .  $\Delta\sigma$  was chosen such that  $\varepsilon = 0.05$ , since, as will be shown in next, this seems to yield the best results.

At first sight, both methods seem to follow the analytic curve quite nicely, however upon examination of the relative error it becomes clear that KDE consistently overestimates the Fisher information by about 40% whereas DEFT has a zero median relative error. Also the spread of the results differ between the two methods. The KDE method has a spread of about 100% of the original value, whereas DEFT has a spread of 30% – 40%. So we see that indeed, DEFT provides an improvement over KDE both in the estimated value and in the error margins. An important technical note: in the above computations, the KDE values were not obtained from Eq. (2) directly, but rather from a version of this where the logarithms were retained. The reason for this was that this gave a result which was orders of magnitude more accurate. DEFT did not benefit from this change and in fact gave slightly worse results (though still better than the KDE results).

For the rest of our computations we use DEFT (with the same parameters as before) for the density estimation. We next investigate the dependence of the estimation error on  $\varepsilon$  at a fixed number of samples  $N = 2 \times 10^4$ . To test this we computed the Fisher information for  $\sigma = 0.5, 1, 2, 5, 10$ . Each computation was repeated 100

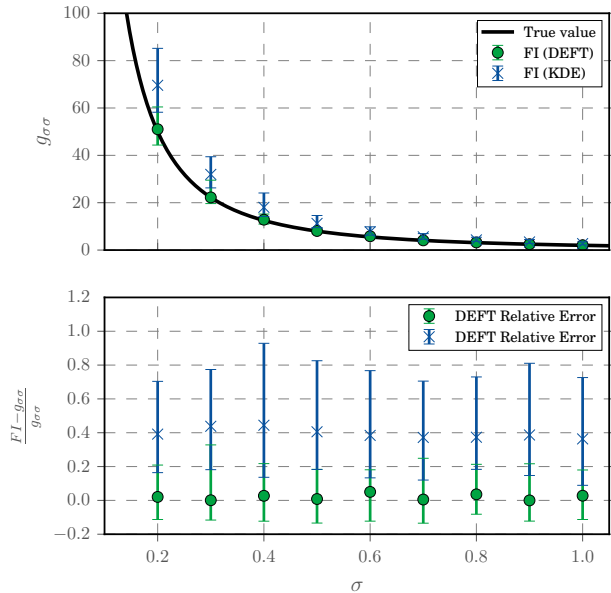


FIG. 2. (Color online) A comparison between using Gaussian KDE and DEFT for the density estimation. Top figure shows the Fisher estimate of both methods. Error bars represent 5 and 95 percentiles. Bottom figure shows the relative errors of both methods. The values were computed with  $N = 10^4$ ,  $\varepsilon = 0.05$ , and 100 repetitions at each  $\sigma$ . The same samples were used by both methods.

times at various values of  $\varepsilon$ . For each set of 100 repetitions we computed the median and the 5 and 95 percentiles of the relative error (defined as the computed value minus the true value divided by the true value). We find that all of the curves seem to have the same functional dependence on  $\varepsilon$ , and that, as we predicted, there is an optimal value for  $\delta\sigma$ , characterized by  $\varepsilon \approx 0.05$ . This means that the errors depend on  $\sigma$  through the combination in Eq. (7), as shown in Fig. 3. The different curves represent the different values of  $\sigma$ . All the curves have a minimum in the range of  $\varepsilon \in [0.04, 0.1]$ . At small  $\varepsilon$  they grow due to errors in the numerical derivative ( $\Delta\sigma$  too large). At large  $\varepsilon$  they grow due to overlapping densities. In between is the range where we get best results. The spread (the 90% inter-percentile range) is minimal at  $\varepsilon = 0.05$  as well. The shaded regions in the plot represent the 90% range of the various  $\sigma$  curves.

To test the dependence on  $N$  and  $\varepsilon$  we varied both and computed  $g_{\sigma\sigma}$ . The result is presented as a heatmap in Fig. 4. The color represents the absolute-value relative estimation error in logarithmic scale. The dashed line indicates the  $\varepsilon = 0.1$  line and the dash-dotted line represents the  $\Delta\sigma = 0.35$  line. All computations were done with  $\sigma = 1.0$  and 100 repetitions. In the figure, the  $\varepsilon = 0.1$  line denotes the highest value of  $\varepsilon$  that still yields good results. The errors due to small  $\Delta\sigma$  seem to follow the  $\varepsilon = 0.1$  curve, showing again the dependence of this type of error on  $\varepsilon$ . Above  $\Delta\sigma = 0.35$  we see increasing errors due to the large value of  $\Delta\sigma$ . The best area for

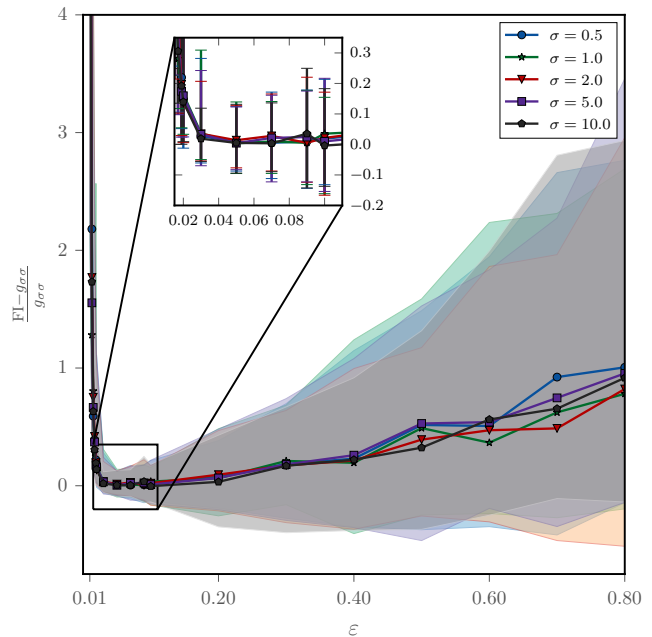


FIG. 3. (Color online) The relative error as a function of  $\varepsilon$  for different values of  $\sigma$ . FI stands for the computed value and  $g_{\sigma\sigma}$  the true value. The dots represent the median relative error in the estimation and the colored areas indicate the 90% inter-percentile range computed over 100 repetitions of the computation. Each value was computed with  $N = 2 \times 10^4$ . The edges of the shaded regions, and the error bars in the inset are the 5 and 95 percentiles.

the estimation is between the two lines.

One of the applications of the computation of Fisher information from samples is in detecting phase transitions [17]. As a further validation for our computation we took the prototypical example of a second order phase transition, namely the two dimensional Ising model. It is a model of binary spins  $s_i$  on a square lattice with nearest-neighbors interaction. Its Hamiltonian is

$$\mathcal{H} = - \sum_{\langle i,j \rangle} J_{ij} s_i s_j - h \sum_i s_i, \quad (10)$$

where  $\langle i, j \rangle$  indicates the sum is on nearest neighbors,  $s_i = \pm 1$  is the value of a spin at site  $i$ ,  $J_{ij}$  is the interaction energy, and  $h$  is an external applied magnetic field. At more than one dimensions there is a critical order-disorder phase transition at a finite temperature. Onsager solved the model exactly in two dimensions in the thermodynamic limit (infinite number of spins) and at zero applied external field [29]. The critical temperature in the isotropic case ( $J_{ij} \equiv J$ ) is

$$T_c = \frac{2J}{\ln(1 + \sqrt{2})} \approx 2.269J. \quad (11)$$

For simplicity we set  $J \equiv 1$  and Boltzmann's constant  $k_B \equiv 1$ .

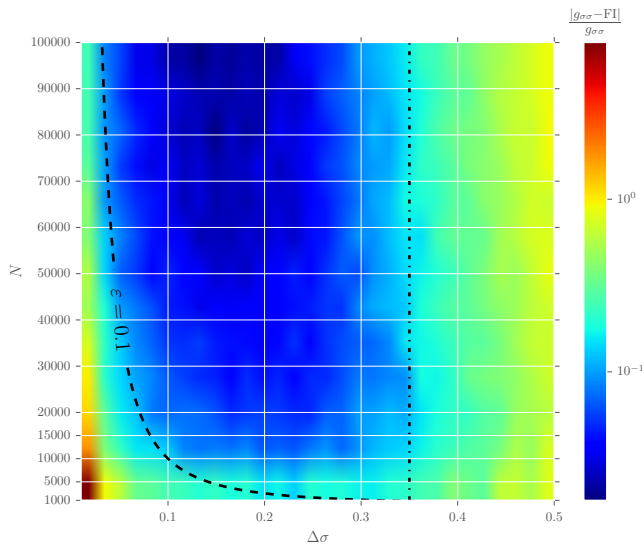


FIG. 4. (Color online) Relative error in the computation of the Fisher information for  $\sigma = 1.0$  as a function of both  $\Delta\sigma$  and  $N$ . Computed using DEFT with 100 repetitions per point. Dashed line represents the  $\varepsilon = 0.1$  line and the dash-dotted line is the  $\Delta\sigma = 0.35$  line. Unlike the previous plots, here we compute the absolute value relative error to avoid problems with the logarithmic color-bar scale.

Prokopenko *et. al.* [17] computed both the  $TT$  and  $hh$  components of the Fisher information (computed for the Gibbs distribution with  $\theta^1 = h$  and  $\theta^2 = T$ ) in terms of the susceptibility  $\chi_T$  and the specific heat  $C_h$  and showed that (temporarily restoring Boltzmann's constant  $k_B$ ):

$$g_{TT} = \frac{C_h}{T^2}; \quad g_{hh} = \frac{\chi_T}{T}. \quad (12)$$

We therefore expect both to diverge as the system approaches the critical temperature. In a finite system this means that the Fisher information peaks at the critical temperature.

To validate this result we simulate the Ising model and compute the Fisher Information. We used the Metropolis-Hastings Monte Carlo algorithm to obtain samples of the configuration energy with the Gibbs distribution (at zero external field):

$$p(S; T) = \frac{1}{Z(T)} \exp[-\beta\mathcal{H}(S, T, h = 0)]. \quad (13)$$

Here  $\beta = 1/T$  is the inverse temperature,  $S = \{s_i\}_{i=1, \dots, L^2}$  is a configuration of the spins on a  $L \times L$  square lattice, and  $Z$  is the partition function. We then estimate the  $TT$  component of the Fisher information using Eq. (2) with densities estimated from the sampled energies. We also computed the specific heat:

$$C_h(T) = \frac{1}{L^2 T^2} (\langle E^2 \rangle - \langle E \rangle^2) \quad (14)$$

where  $L^2$  is the total number of spins,  $E$  is the energy

of the configuration, and the average is performed over different configurations at the same temperature.

We plot the result of both the Fisher information and the specific heat  $C_h$  computation in Fig. 5. The simulation was run on a  $25 \times 25$  lattice of spins with periodic boundary conditions in the temperature range  $[0.5, 4.0]$  which we divided into 200 segments, leading to an increment of  $dT \simeq 0.17$ . We repeated the simulation with different random initial conditions 5 times to show the median and 5 and 95 percentiles. We used a warm-up period of  $5 \times 10^6$  time steps and took  $N = 15,000$  samples of the configuration energy. We then estimated the probability density from the 15,000 samples using DEFT (with  $G = 200$ ,  $\alpha = 3$  and a bounding box of  $[-4, 1]$ ) and computed the Fisher information. Because the Fisher information varies,  $\varepsilon$  was not constant. Its median was  $\varepsilon = 0.12^{+0.12}_{-0.07}$  for the values of  $\varepsilon$  which were not infinite (the error margins were computed for the 5 and 95 percentiles). To verify that Eq. (12) holds, we plot the ratio of the two sides of the equation. This is presented in the inset in Fig. 5.

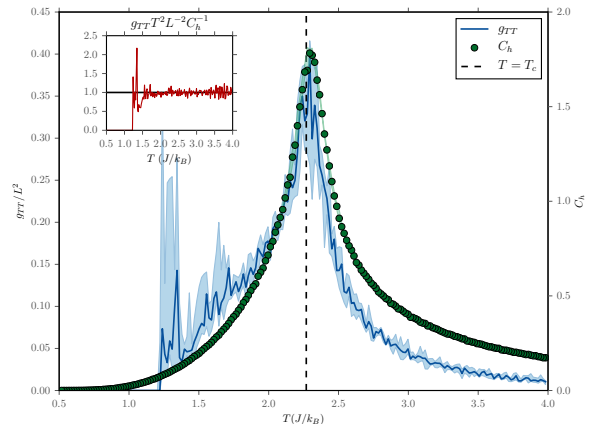


FIG. 5. (Color online) Blue continuous curve is the  $TT$  component of the Fisher information matrix in the  $2D$  Ising model on a  $25 \times 25$  grid. Shaded blue region indicates the 5 and 95 percentiles computed from 5 simulations. Green dots are the heat capacity computed from the same samples. Shaded green region is again the 5 and 95 percentiles. Inset shows the ratio of Fisher information to heat capacity (more specifically  $g_{TT} T^2 C_h^{-1} L^{-2}$ ) which according to Eq. (12) should be 1.

There are several technical points we would like to mention about the implementation of the method. First, we performed the same computation with a smaller grid spacing ( $dT = 0.007$ ). This led to a much worse signal-to-noise ratio because the very close densities caused large peaks to occur, especially in the low temperature range. Second, it is important to find the most suitable parameters for DEFT. If the bounding box is too small, or the number of grid points too small or too large, the estimated density will have multiple peaks which are not apparent in the data. Thus we recommend plotting the result of DEFT together with a histogram for several data points to make sure the convergence is good. Third, in

the computation of Eq. (2) the term  $1/p$  may contribute large values at very small  $p$ . Equivalently, if the Fisher information is computed directly with the logarithms in Eq. (1), when  $p(x|\theta \pm \Delta\theta)$  are small, their logarithm will again be large. This requires the introduction of a numerical cut-off. It is common practice to set the contribution of a term where  $p(x) = 0$  to zero [18]. We thus introduced a cut-off such that if any of the estimates at a particular point is zero, the contribution of this point to the integral will be zero. We investigated the effect of this cutoff for a range of values between  $10^{-20}$  and  $10^{-2}$ . The value of the cut-off had very little effect. In the Ising model, the only effect was to change the size of the low temperature region where the Fisher information is exactly zero (the lower the cutoff, the smaller the region was). In producing Fig. 5 we used a value of  $10^{-10}$ . Lastly we would like to mention that the plots in Fig. 5 were obtained by the use of logarithms instead of Eq. (2).

As is clear by the remarks above, care should be taken when using this method to compute the Fisher information. One should first make sure a good convergence of DEFT is achieved, by adjusting  $G$ ,  $\alpha$  and the bounding box. Then make sure to select the correct parameter difference  $\Delta\theta$ , a decision that can be aided by the estimation of the  $\varepsilon$  parameter. And also, if necessary, use a cut-off for very low values of the probability density. Since we rely on DEFT to perform the density estimation,

the procedure is limited by the limitations of DEFT. It is especially important to note that so far DEFT has been implemented in 1 and 2 dimensions. Higher dimensions suffer from the ‘‘curse of dimensionality’’ since they require exponentially many grid points to evaluate the density.

OHS would like to thank Joan Massó and Antoni Arbona from the University of the Balearic Islands for enlightening discussions. Some of the simulations for the Fisher information computation in the Ising model were performed using the Computational Exploratory being developed at the University of the Balearic Islands. This research was supported by the Future and Emerging Technologies (FET) programme within the Seventh Framework Programme (FP7) for Research of the European Commission, under the FET-Proactive grant agreement Sophocles, number FP7-ICT-317534 and the Future and Emerging Technologies (FET) programme within the Seventh Framework Programme (FP7) for Research of the European Commission, under the FET-Proactive grant agreement TOPDRIM, number FP7-ICT-318121. AgH wishes to acknowledge partial funding by the Russian Scientific Foundation, under grant #14-11-00826. PMAS wishes to acknowledge partial funding by the Russian Scientific Foundation, under grant #14-21-00137

- 
- [1] T. M. Cover and J. A. Thomas, *Elements of Information Theory* (John Wiley & Sons, 2006) p. 640.
- [2] S.-I. Amari and H. Nagaoka, *Methods of Information Geometry; Translations of mathematical monographs, Vol. 191* (American Mathematical Society, 2000).
- [3] G. Ruppeiner, Phys. Rev. A **20**, 1608 (1979).
- [4] G. Ruppeiner and C. Davis, Phys. Rev. A **41**, 2200 (1990).
- [5] G. Ruppeiner, Rev. Mod. Phys. **67**, 605 (1995).
- [6] G. Ruppeiner, a. Sahay, T. Sarkar, and G. Sengupta, Phys. Rev. E **86**, 052103 (2012).
- [7] R. Ingarden, H. Janyszek, A. Kossakowski, and T. Kawaguchi, Tensor (NS) **37**, 105 (1982).
- [8] H. Janyszek and R. Mrugala, Phys. Rev. A **39**, 6515 (1989).
- [9] H. Janyszek, J. Phys. A: Math. Gen. **23**, 477 (1990).
- [10] D. Brody and N. Rivier, Phys. Rev. E **51**, 1006 (1995).
- [11] D. C. Brody and D. W. Hook, J. Phys. A: Math. Theor. **42**, 023001 (2009).
- [12] P. Kumar, S. Mahapatra, P. Phukon, and T. Sarkar, Phys. Rev. E **86**, 051117 (2012).
- [13] T. Obata, H. Hara, and K. Endo, Phys. Rev. A **45**, 6997 (1992).
- [14] T. Obata, H. Oshima, and H. Hara, Phys. Rev. E **56**, 213 (1997).
- [15] A. L. Mayer, C. W. Pawlowski, and H. Cabezas, Ecol. Modell. **195**, 72 (2006).
- [16] S. A. Frank, J. Evol. Biol. **22**, 231 (2009).
- [17] M. Prokopenko, J. T. Lizier, O. Obst, and X. R. Wang, Phys. Rev. E **84**, 041116 (2011).
- [18] X. R. Wang, J. T. Lizier, and M. Prokopenko, Artif. Life **17**, 315 (2011).
- [19] J. Hidalgo, J. Grilli, S. Suweis, M. a. Muñoz, J. R. Banavar, and A. Maritan, Proc. Natl. Acad. Sci. U. S. A. **111**, 10095 (2014).
- [20] B. W. Silverman, *Density estimation for statistics and data analysis*, Vol. 26 (CRC press, 1986).
- [21] E. Walter and L. Pronzato, *Commun. Control Eng.* (Springer Verlag New-York, 1997).
- [22] W. Bialek, C. Callan, and S. Strong, Phys. Rev. Lett. **77**, 4693 (1996), arXiv:9607180v1 [arXiv:cond-mat].
- [23] J. B. Kinney, Phys. Rev. E **90**, 011301 (2014).
- [24] P. J. Huber, Ann. Stat. **2**, 1029 (1974).
- [25] L. Kostal and O. Pokora, Entropy **14**, 1221 (2012).
- [26] I. Goodd and R. Gaskins, Biometrika **58**, 255 (1971).
- [27] I. N. Sanov, Mat. Sb. **42(84)**, 11 (1957).
- [28] This well-known result can be derived using a Taylor expansion and the definition of the Fisher information.
- [29] L. Onsager, Phys. Rev. **65**, 117 (1944).